Int. J. Electrochem. Sci., 8 **(2013)** 4384 - 4396

International Journal of
ELECTROCHEMICAL
SCIENCE
www.electrochemsci.org

Electrochemical Impedance Spectroscopy Behaviour of Guanine on Nanostructured Planar Electrode

Radim Hrdy[1,2], Hana Kynclova[1], Jana Drbohlavova[1,2], Vojtech Svatos[2], Jana Chomoucka[1,2], Jan Prasek[1,2], Petra Businova[1,2], Jan Pekarek[1,2], Libuse Trnkova[1,3], Rene Kizek[1,2], Jaromir Hubalek[1,2]

[1] Central European Institute of Technology, Brno University of Technology, Technicka 3058/10, CZ-616 00 Brno, Czech Republic, European Union
[2] Department of Microelectronics, Faculty of Electrical Engineering and Communication, Brno University of Technology, Technicka 3058/10, CZ-616 00 Brno, Czech Republic, European Union
[3]Department of Chemistry Faculty of Science, Masaryk University, Kamenice 5, CZ-625 00 Brno, Czech Republic
[*]E-mail: hrdy@feec.vutbr.cz

Received: 1 September 2012 / *Accepted:* 30 October 2012 / *Published:* 1 April 2013

The aim of this work is the optimization and following characterization of gold nanostructured electrochemical sensors suitable for biomolecules and heavy metal ion detection. Gold nanoparticles need to be examined for biocompatibility and environmental impacts. The EIS (electrochemical impedance spectroscopy) measurements of surfaces with various nanoparticles geometry have shown a strong dependence of active electrochemical surfaces area on the rate of nanomachining. The main aim of the paper presented is discovery of planar nanostructured electrode with selected size of nanoparticles which can bring greater benefit in their application in biochemistry in comparison to a flat gold electrode. The cyclic voltammetry method has prooved that nanowires with selected aspect ratio have increased electrochemicaly active area of electrodes.

Keywords: Electrochemistry, Electro-impedance Spectroscopy, Cyclic Voltammetry, Gold Nanoparticles, Biosensor, Guanine

1. INTRODUCTION

Electrochemical high resolution of heavy metal ions such as $Pb^{2+,}$ Hg^{2+} or Ag^{+} [1, 2] or DNA electrochemical fragment detection can be improved by nanostructured surface of electrochemical sensors [3-5]. The main idea of using nanoparticles in microelectronic devices is enlarging the active surface of very small working electrodes and gaining some special new abilities such as higher selectivity and signal stability [6, 7]. Some of the most well-known and frequently used methods to

synthesize metal nanoparticles include wet chemical synthesis of spherical nanoparticles, physical or chemical vapour depositions of nanorods and electrochemical growth of nanowires through highly ordered nanoporous template, which is used in our work [7-12]. However, the metal nanowires on the electrode surfaces improving their detection ability are not always easy to obtain. According to the previous papers related to this issue, the nanostructures, especially long nanowires, covering the electrode surface do not always provide improved detection limit and sensitivity in comparison with flat electrodes without nanoparticles [13]. The responses of nanostructured sensors to analyst are usually worse which is caused by the ions interacting only with the top parts of nanowires. One of the solutions is the change of nanowire geometry and simultaneously the parameters for diffusion layer forming.

When the electrodes are immersed in the solutions, the diffusion layer is created on the electrode/liquid interface. The surface potential of electrode draws up the ions from the solution and causes the formation of diffusion layer as well as the charge transfer resistance and double layer capacity. These are crucial parameters describing the influences of the electrochemical performance on the nanostructured electrodes [14]. Some studies have shown the fact, that non flat electrodes, namely nanostructured electrodes, have diffusion layer composed from many semi-spherical parts belonging to each independent nanostructure. In one case, if these semi-spherical diffusion layers are separated or their overlap is less than half of diffusion layer radius, the effect of nanostructures is very significant [15].

It means the interactions can proceed on the whole electrode surface [16, 17]. Each nanostructure participates in electrochemical reactions. In another case, if the overlap is higher, the electrode can behave like flat electrode. It is supposed that only segments of the surface can participate in the electrochemical reactions [18, 19].

In that aspect, electrochemical impedance spectroscopy (EIS) is a powerful tool in characterizing an electrode nanostructured surface and understanding the electrochemical processes on it [20]. Many studies reported on the investigation of electrochemical interactions on nanostructured (carbon nanowires, nanoporous, and organic nanocomposed material, etc.) working electrode by EIS technique [21-23]. Moreover, we can demonstrate that the total impedance of a nanostructured working electrode with metal nanowires is changed with modifications of nanowire geometry. In order to fully understand the processes on the surface, it is possible to employ not only EIS but also voltammetric and electron microscopic methods. Especially cyclic voltammetry can be very helpful for determination of the real active surface of a nanostructured electrode, which does not correspond to the geometrical size of the electrode. [24, 25].

2. EXPERIMENTAL PART

2.1. Chemicals

Titanium (99.99%, Goodfellow, UK), aluminium (99.999%, Goodfellow, UK), oxalic acid ($C_2H_2O_4.2H_2O$, 99.5%, p., Penta, CZ), potassium sulphate (K_2SO_4, p., Lachema-Neratovice, CZ), potassium dicyanoaurate ($K[Au(CN)_2]$, 68%, Safina, CZ), boric acid (H_3BO_3, p., Penta, CZ),

phosphoric acid (H_3PO_4, 98%, p.a., Penta, CZ), potassium ferricyanide ($K_3Fe(CN)_6$, 99%, Sigma Aldrich, USA), potassium chloride (KCl, 99.95%, p.a., Penta, CZ), ammonium hydroxide (NH_4OH, 25%, p.a., Fluka, Germany) and guanine (98%, Sigma Aldrich, UK) were used as purchased without any purification. Deionised water was obtained from Millipore RG system MiliQ (Millipore Corp., USA, 18.2 MΩ). The scan electron microscopic observing was perform on pure Al 99.999 % stubs and silver paste (Agar corp, UK).

2.2. Electrodes and Nanostructured Surface Fabrications

Measuring electrodes have been fabricated by electrochemical synthesis. In our work, the platinum electrodes modified with gold nanowires have been used [26]. The thin titanium layer of 20 nm was evaporated on silicon wafer and subsequently the platinum layer of 200 nm and aluminum film of 1 μm were deposited on the titanium one.

The aluminum layer has been transformed by anodic oxidation, so called anodization, to hexagonally ordered porous alumina template [27]. The thin porous anodic alumina template has been obtained by one-step anodization process under constant voltage (40 V) in 0.3 M oxalic acid at 17 °C. The counter electrode was a gold one. The pores in the alumina layer have been organized to honeycomb structures, perpendicular to conductive bottom layer. Subsequently, the porous template has been filled with gold to obtain the nanostructures, e.g. nanowires [28]. For controlled formation of the gold nanostructures, a simple electrochemical reduction of gold ions was used according to recent papers [27, 29]. The electrolyte used consists of 6 $g.L^{-1}$ potassium dicyanoaurate and 2.32 $g.L^{-1}$ boric acid. The nanowires have been formed on conductive bottom layer according to porous geometry. The length of nanowires was determined by deposition time and current density. The time was 5 seconds, the current density of deposition was usually 0.25 $mA.cm^{-2}$. The alumina template was dissolved in 5% phosphoric acid. Finally, the electrodes were rinsed in demi water and the platinum electrodes with gold nanowires have been obtained [30].

2.3. Electrochemical Impedance Spectroscopy

Measuring system Metrohm μAutolab III with FRA2 module supported by NOVA 1.8 software was used for the EIS characterizations of electrodes. Samples were measured in 10 ml of potassium sulphate of various concentrations (0.1 μM – 10 mM). The frequency range was set to 1 Hz – 1 MHz and the amplitude was 60 mV We observed the signal perturbations on low amplitude less than 40 mV. The value of 60 mV was chosen according to a previous measurement for its higher system stability compared to measurement at low frequency in the range of 1–100 Hz.. The EIS experiments were carried out in potentiostatic regime under DC zero potential related to reference electrode. The effect of a parasitic capacitance or inductance usually observed at high frequencies was shielded in Faraday cell. For the EIS experiment a three electrode cell with Pt auxiliary electrode and Ag/AgCl/3M KCl reference electrode was used.

2.4. Electrochemical Impedance Spectroscopy of Guanine

The EIS of guanine in potassium sulphate solution was measured. Measuring conditions, such as quantity of buffer solution, frequencies, amplitude or potential of signal, were used the same as in the previous case. The gradual additions of guanine in amount of 100 µl and concentration of 0.8 mM were added to the solution to obtain various concentrations, such as 16 , 31 , 45 , 60, 73 , 86 and 100 µM. Each electrode and additions were accumulated for 4 minutes. The fabricated nanostructured electrode was tested in pure electrolyte and after the test we performed the EIS measurements of solutions with guanine added.

2.5. Cyclic Voltammetry

Measuring system Metrohm µAutolab III with FRA2 module supported by NOVA 1.8 software was also used for the cyclic voltammetry (CV) characterization of electrodes. The platinum electrode was used as a counter electrode. The Ag/AgCl/3M KCl was used as a reference electrode. The measurements were carried out in potassium chloride of 0.1 M with additions of potassium ferricyanide of various concentrations (2.5 , 5 mM and 7.5 mM) [31]. Concentration of potassium chloride was chosen according to the known value diffusion coefficient of 6.5×10^{-6} $cm^2.s^{-1}$. The measurement was performed at several scan rates ranging from10 to 50 $mV.s^{-1}$.

3. RESULTS AND DISCUSSION

3.1. Structural characterizations

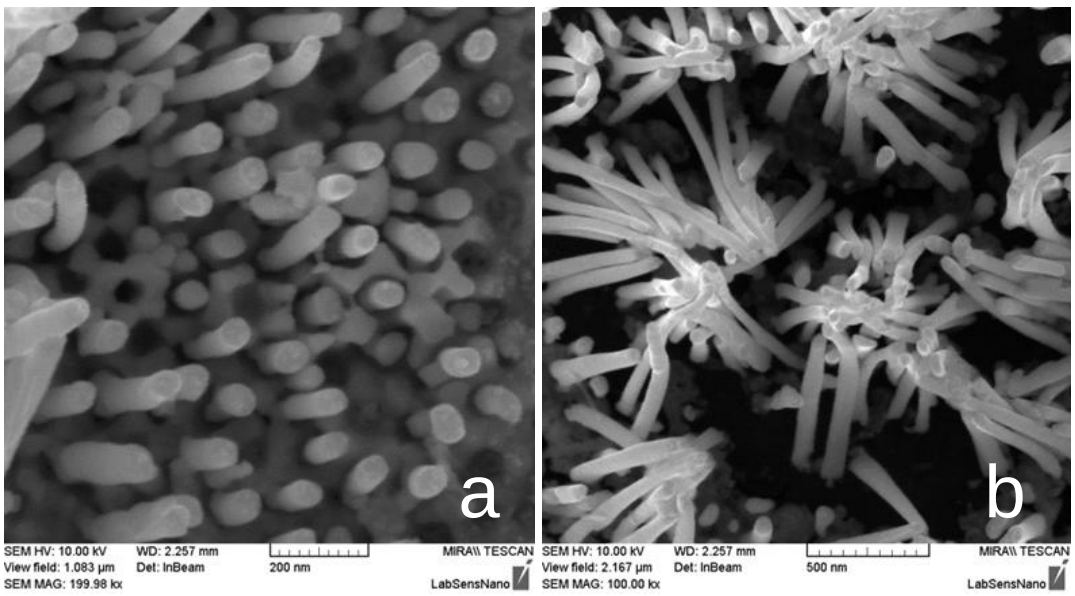

Figure 1. Gold nanorods in porous alumina template (1a). The submicron clusters with over deposited nanowires without template (1b). All SEM observing was performed under high vacuum mode 10^{-4} Pa, accelerating voltage 10 kV and magnification 200 kx (1a) resp. 100 kx (1b). The work distance of InBeam detector was 2.25 mm.

The Figures 1a and 1b from SEM analysis show briefly the fabrication process. The non-completely removed nanoporous alumina template with pore diameter of about 50 nm can be seen in Figure 1a. These pores are filled with gold to form nanowires. After the total dissolving of template, the perpendicularly standing nanowires are obtained. However, if the length becomes overly high (high aspect ratio), the nanowires can lose self-stability. Then, the electrode surface will be covered by submicron clusters composed of clumped nanowires, which is presented in Figure 1b.

Three ring types of gold electrodes with diameter of 3 mm and two different surface nanostructures have been fabricated. The comparative flat electrode was fabricated as a pure evaporated gold surface. The first type of nanostructured electrode was obtained under lower deposition current density of 0.5 mA resulting in reduced nanowire length and obtained lower aspect ratio. The second type was fabricated under current density of 5 mA, where the deposition time was determined to fill alumina template with metal and obtain nanowires with a length close to hundreds of nanometres. The comparison of diameter and length of nanowires gives the aspect ratio more than 1:10. The same time was applied under lower current deposition, where the nanowires, in this case rather nanorods, have the height up to one hundred nanometres [32]. The aspect ratio of nanorods was about 1:3. In both cases, the whole surface has homogenous coverage by nanoparticles. Some, gaps and boundaries are visible, being caused by crystals or impurities in the template. As seen in figures 2a and 2b, both surfaces have different nanowire distribution. The electrode prepared at lower depositions current has sparse distribution, i.e. density of nanowires. The lower deposition current has caused the smaller ratio between diameter of nanorods and their distance in comparison with the other type. According to recent works, the time of deposition was the only factor which affected the length of nanowires without any effect on distribution. We observed the direct proportion between these factors.

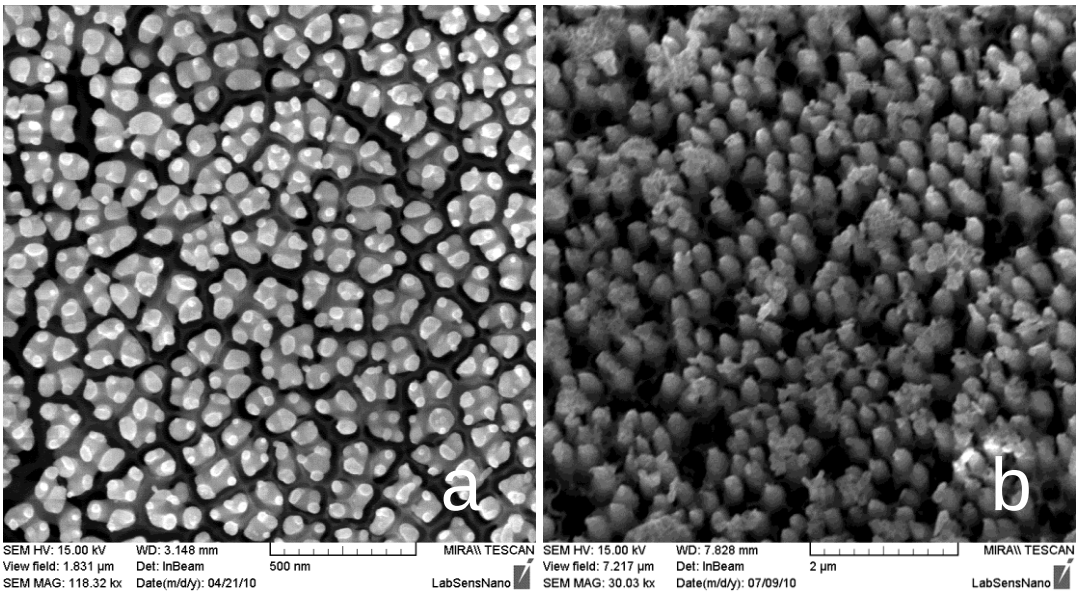

Figures 2. Gold nanorods with low surface distribution with significant crystal boundaries (2a) and long gold nanowires (2b). SEM observing was performed under high vacuum mode 10^{-4} Pa, accelerating voltage 15 kV and magnification 100 kx (2a) resp. 30kx (2b). The work distance of InBeam detector was 3.1 mm (2a) resp. 7.8 mm (2b).

3.1. EIS characterization

The basic characterizations were performed in potassium sulphate for its stability. There is an additional benefit to this compound, since it does not create the complexes with gold in comparison with potassium chloride. This creation of gold-chloride complexes can violate the surface homogeneity and disturb the exact measurements. The comparisons of these three types of electrodes have brought many interesting observations of differences in electrode behaviour. EIS spectra corresponding to each electrode can be seen in Figure 3. Both nanostructured types have a similar sort of diffusion part, which means the same angle in comparison with the flat surface without nanostructures. However, shorter diffusion parts of the impedance locus of nanostructured electrodes indicated the shift of total impedance in frequency spectra [33]. There is also some non-linearity in diffusion parts especially in nanostructured electrodes, which are visible as the beginning of secondary semicircle These secondary semicircles cause decreasing the angle of diffusion part much less than 45° which is typical for Warburg on the flat electrode. The effect of semicircles is corresponding to the effect of nanomachinig, showing the additional capacitance as well. It must be calculated in following simulations. However, a small similar effect can also be seen on the flat electrode. The diffusion part is not absolutely straight. It could be caused by sub nanomachining or crystalinity of the gold film.

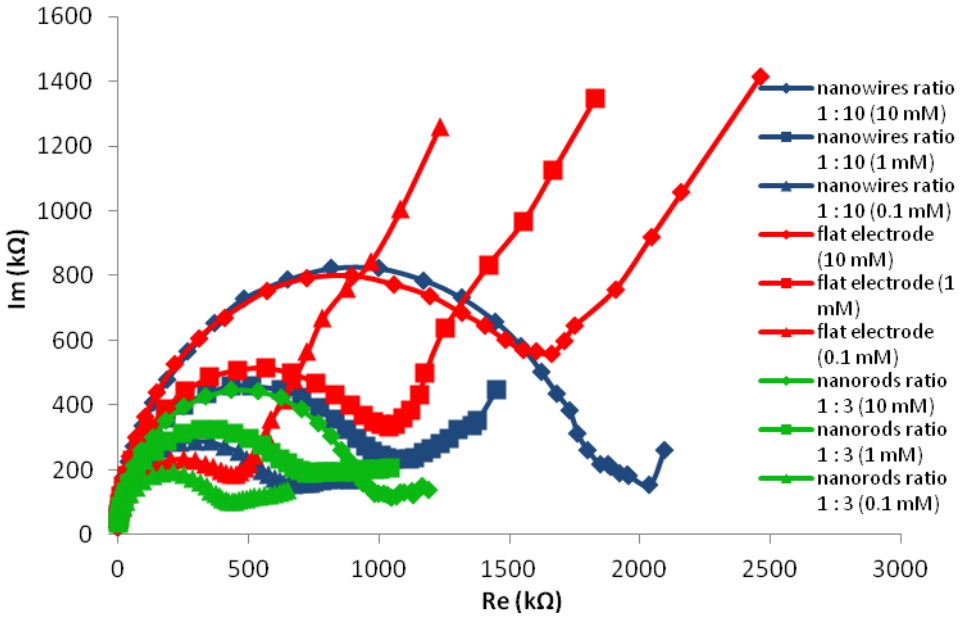

Figure 3. EIS spectra of nanorods, nanowires and nanostructure free surface measured in potassium sulphate. The frequency range was set on 1 Hz up to 1 MHz and the amplitude was 60 mV.

The following simulation of double layer capacity C_{dl} was calculated from the simulation according to equivalent circuit, seen in Figure 4. All simulations were performed in MetroOhms EcoChemie software, which is a part of NOVA soft. The equivalent electrical circuit was chosen according to recent studies [34]. The basic Radels circuit was modified by second parallel C/R element, related to additional capacitance of nanostructures. The next adaptation was swapping the Warburg element to Constant Phase Element CPE [35]. Usage of CPE model brings more benefits in

simulations and it is necessary for describing electrochemical reactions on electrodes and calculations of capacitance [36]. If we compare the effect of double layer capacity, which is represented by semi-circle part of graphs, the differences between nanostructures are significant. The remaining part of nanowires with aspect ratio 1:10 surface is very similar to that of the flat surface. The value of double layer capacity and charge transfer resistance are equal. In these cases, we can determine the corresponding size of active electrochemical area. The nanowires with aspect ratio 1:3 have less impact on increasing the electrode surfaces as expected. On the other hand, short nanorods had ten times less impedance than the rest of them which showed that the real electrochemical surface area had been increased. Obviously, shorter nanorods have higher impact on forming the diffusion layer. It indicates that the aspect ratio of nanowires is of a great importance.

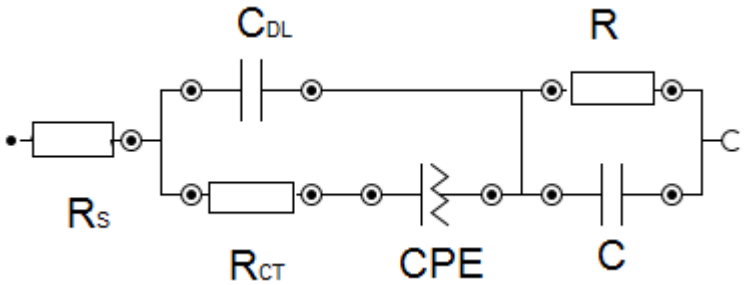

Figure 4. Equivalent electrical circuit model for coating EIS spectra dealing with nanostructured electrodes. R_S is the solution resistance. The constant phase element, C_{dl} is then related to the space charge capacitance at the guanine–electrolyte interface. R_{ct} is related to the charge transfer resistance at the guanine–electrolyte interface. The constant phase element CPE is the Warburg impedance due to mass transfer to the electrode surface. R and C is additional capacitance element of nanostructures.

One of the possibilities how to determine the differences between electrodes is the charge transfer R_{ct} comparison. The R_{ct} values are impedance lower limits and they have been counted out from measured data and separated, as shown in Figure 5a. These impedance lower limits have appeared at the point corresponding to the interface between the diffusion part at low frequencies and the beginning of more significant influence of double layer capacity which is represented by the semi-spherical parts of impedance spectres. These impedance lower limits are usually visible at a frequency range of 1.5–3 kHz. The value of limit is a result of a count of the charge transfer resistance R_{ct} and the impedance of solution R_s. If the value of R_s is always equal to each concentration, R_{ct} is the only variable and significant part of impedance, which can be used for descriptions of electrode surface behaviour. The different behaviour of surfaces covered with short nanorods can be seen in Figure 5a. It is clear that the R_{ct} of electrode with nanorod surface is ten times lower than other systems and it has a linear progress. However, this phenomenon has appeared only at low concentrations, up to 100 μM of potassium sulphate. At higher concentrations, the values became much closer. According to this investigation, the value of a double layer capacity C_{dl} was simulated in NOVA 1.8 software (MethroOhm) as can be seen in Figure 5b. We found out that the C_{dl} has a nonlinear course. Moreover,

the significant transcend of nanostructured surface is only visible in a very narrow range of concentrations, from 0.1 to 100 μM of potassium sulphate.

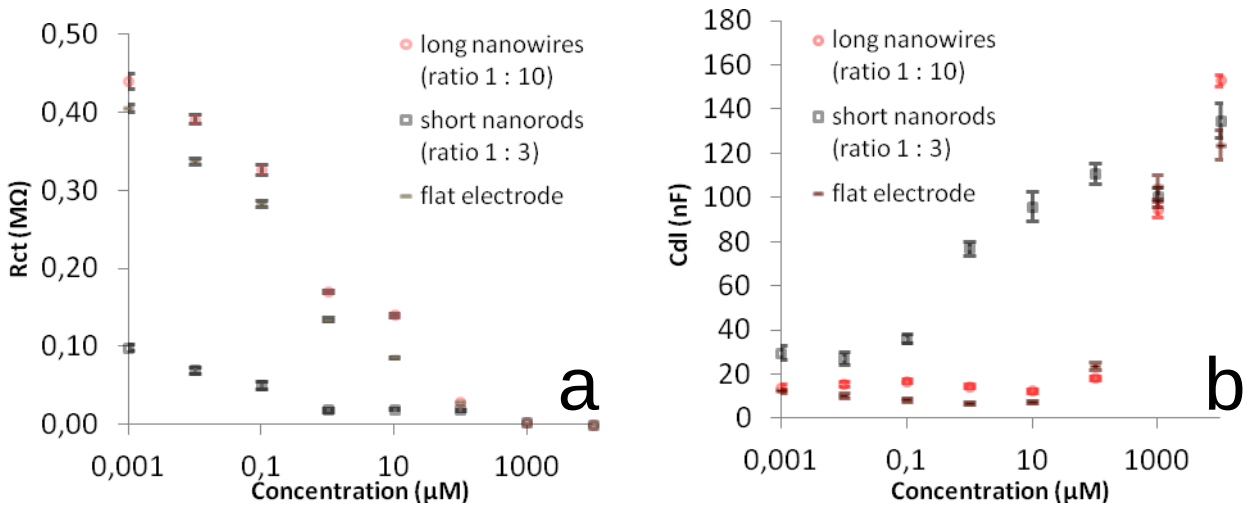

Figures 5. The dependence of impedance minima of spectra (separated Rct) on concentrations of potassium sulphate supported by relatively standard deviation RSD calculated to value less than 2.35. (4a). The dependence of double layer capacity (C_{dl}) on concentrations on potassium sulphate supported by relatively standard deviation RSD calculated less than 9.85 on the highest value of C_{dl} (4b).

3.2. Nanostructured Electrode Behaviour of Guanine Detection

The nanostructured electrode also has to be characterized from the point of view of detection limit and the nanosurfaces have to be tested for possibilities of measuring the impedance of biomolecules as well [37]. This measurement was performed in guanine solutions for its higher electro reactivity (compared to other four purine bases) with alkylating agents, hydroxyl radical transitions-metal complexes and other oxidants [38, 39]. The effect modification of the working electrode was discussed in recent studies. The EIS measurements of guanine were performed on various types of electrodes (glassy carbon, electrode modified by nanostructures) [40, 41]. Some paper has proved the EIS as a better tool for detection of biomolecules adsorption on the electrode surface than the differential pulse voltammetry. In this case, the EIS was used for detection of impact of guanine adsorption on C_{dl} of a nanostructured surface. Guanine is a dissoluble material, especially in aqueous solutions. Therefore, it has been dissolved in 3 mL of ammonium hydroxide solution. However, the conductivity of final electrolyte was slightly higher [42, 43].

There is a precondition, measured biomolecules served as electron transmitters. In case of higher concentration of biomolecules in solution it is predicted that the biomolecules completely cover the nanostructured electrode because of high affinity to gold. Therefore it is expected to measure only the impedance of biomolecules instead of the measurement of impedance count corresponding to flat electrode and biomolecules. During gradual addition of guanine to electrolyte (ammonium hydroxide

solution) until the concentration reached the value of 86 µM, the impedance R_{ct} decreased to a relatively constant value, as shown in Figure 6, and C_{dl} stepped to 88.6 nF. The next change of double Cdl has been much smaller than the previous value addition, as seen in Table 1.

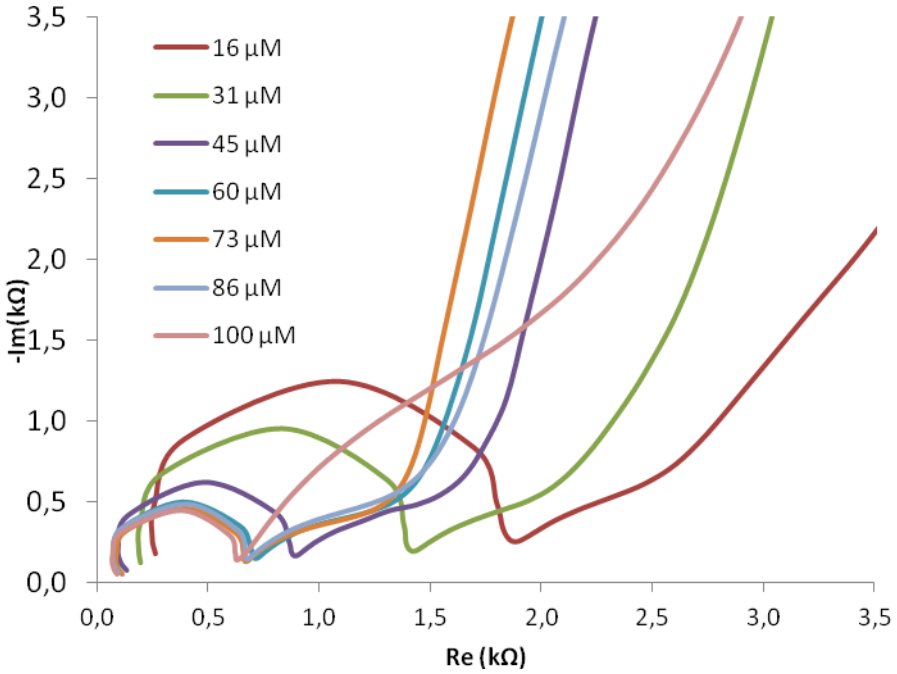

Figure 6. Nyquist plots of fabricated nanostructured electrodes in different guanine concentrations in 0.1 M potassium sulphate buffer. The Nyquist plot on 100 µM corresponds to the concentration of complete surface adsorption of guanine.

Table 1. EIS data obtained from fitting the experimental results to nanostructured surfaces with nanorods of various guanine concentrations for equivalent Randles circuit (see Inset of Figure 6).

c [µM]	R_s [Ω]	C_{dl} [nF]	R_{ct} [kΩ]	CPE [nMho]	CPE [n]	R [kΩ]	C [pF]
0	455	6.65	11	431	0.82	10.5	146
16	207	23.5	2.79	683	0.797	2.64	699
31	144	31.1	2.49	844	0.79	1.9	929
45	106	40	1.89	952	0.779	1.27	1500
60	101	57	1.56	1210	0.766	1.08	1510
73	80.9	72	1.63	1740	0.72	0.754	2240
86	70.9	88.6	1.56	1960	0.729	0.76	2170
100	65.8	93	1.4	2330	0.716	0.781	2190

Data were calculated according to the equivalent circuit in chapter 3.1. At this point, the electrolyte surface seemed to be saturated, i.e. completely covered with guanine molecules and the next addition of guanine had no significant effect on double layer capacitance. The surface is

completely adsorbed by guanine molecules. The remaining free molecules in solution have only affected the diffusion, which always depends on concentration. It can be seen at the highest concentration of 100 µM. The diffusion course was significantly changed. Recent works just study the lowest detection limit, which is reported in the range of nM [5, 44]. In this work the upper concentration limit which is possible to be measured using standard method of the electrochemical impedance spectroscopy has been found. EIS has demonstrated the different behaviour of the electrodes surface after full adsorption of guanine, Compare with nanostructured electrodes, the full adsorption has never been observed on the flat electrodes. At this point, it is possible to directly measure the biomolecules impedance reps. the impedance of biomolecules film adsorbed on the surface as has been theoretically presented [4, 44].

3.3. Cyclic voltammetry measurement of nanostructures

Regarding the increase of electrochemically active surface, it is important to use a sophisticated method for the determination of active surface size [45]. On the basis of cathodic and anodic peak heights and the scan rates of cyclic voltammetry, the active surface can be calculated according to Randles-Sevcik equation [46]. Potassium ferricyanide, which was chosen as a model compound in our work, can exhibit a pair of reversible peaks on voltammetric curves (Figure 7). When scan rate changed from 10 to 50 $mV.s^{-1}$, the anodic peak current was linear to its square root. The diffusion coefficient (D) of potassium ferricyanide was 6.5×10^{-6} $cm^2.s^{-1}$ in this case and the active area of nanorods covering the electrode surface was estimated to be about 0.14 cm^2. It was larger than the effective area of the flat gold electrode (approximately 0.072 cm^2) as well as the electrode with long nanowires with aspect ratio 1:10 (approximately 0.069 cm^2). In the next Figure 8, the relation of the anodic peak to scan rate has been demonstrated in several potassium chloride concentrations. The calculated correlation coefficient is better than 0.99.

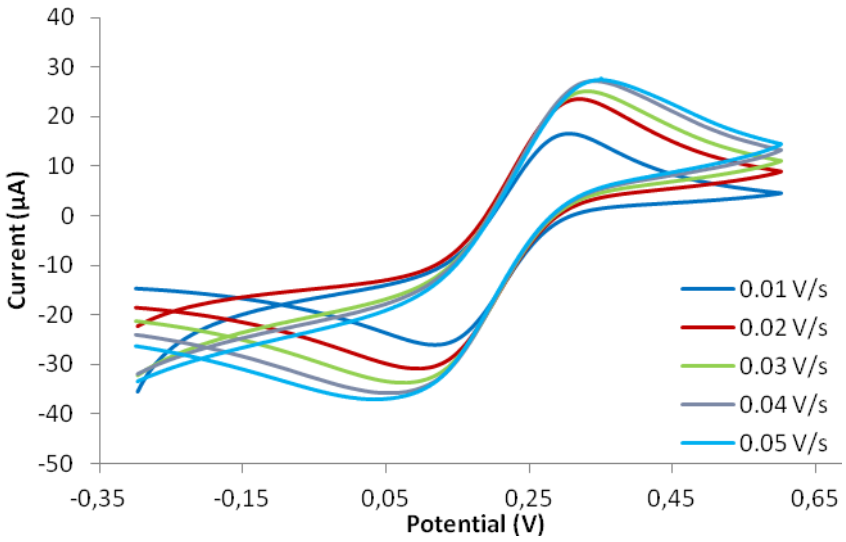

Figure 7. Cyclic voltammetry characterization of short nanorods in various scan rates in 5 mM potassium ferricyanide.

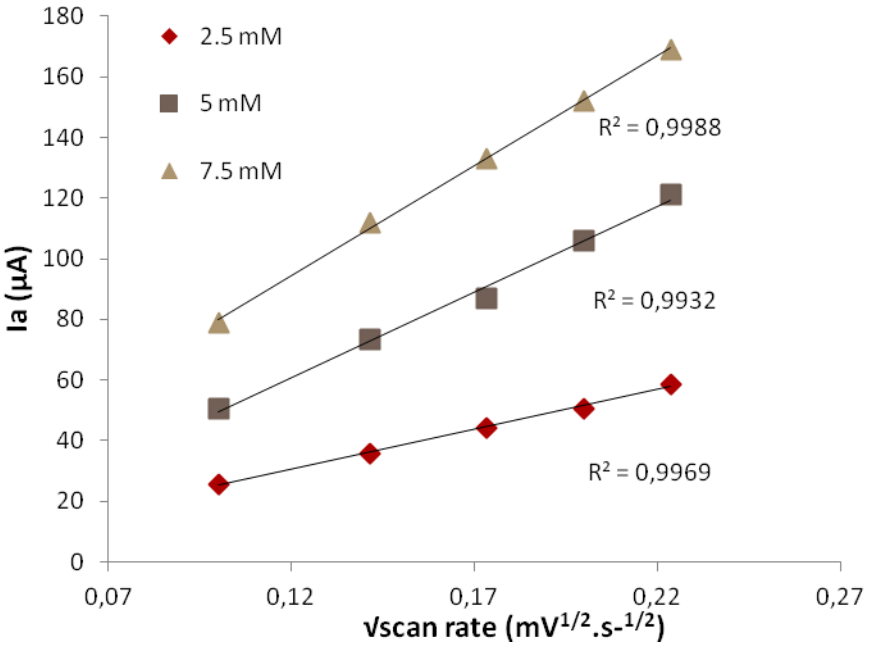

Figure 8. Relation of the anodic peak current on the scan rate square root with calculated correlation coefficient.

4. CONCLUSION

In this paper, we succeeded in significantly improving the sensor active area using a smart method of gold nanowires/nanorods deposition. The direct proportion of the nanowire length and active surface area enlarging has limits. Therefore, we found the optimal conditions for nanowire preparation regarding their length (height) and geometry in order to reach the highest increase of active surface area.

The prepared nanostructured electrodes were also characterized using EIS and cyclic voltammetry methods to find the potential upper detection limit for bioapplications. It has been investigated that the nanostructures are useful for the detection of guanine even in low concentrations. We suppose the method described for the determination of nanostructured electrode detection limit is also suitable for a broad scale of biomolecules. However, there are still some issues which need further investigation to clearly understand this phenomenon.

ACKNOWLEDGEMENT
The work has been supported by IMINAS GA CR 102/09/1601, NANIMEL GA CR 102/08/1546 and CEITEC CZ.1.05/1.1.00/02.0068.

References

1. Kang, T., S.M. Yoo, M. Kang, H. Lee, H. Kim, S.Y. Lee, and B. Kim, *Lab Chip*, 2012. 12(17): p. 3077-3081.
2. Zhang, P., G. Xu, J. Lv, J. Cui, Z. Zheng, and Y. Wu, *J Electroana Chem*, 2012. 685(0): p. 91-96.
3. Gasparac, R., B.J. Taft, M.A. Lapierre-Devlin, A.D. Lazareck, J.M. Xu, and S.O. Kelley, *J. Am. Chem. Soc.*, 2004. 126(39): p. 12270-12271.
4. Grieshaber, D., R. MacKenzie, J. Voros, and E. Reimhult, *Sensors*, 2008. 8(3): p. 1400-1458.

5. Castillo, G., L. Trnkova, R. Hrdy, and T. Hianik, *Electroanalysis*, 2012. 24(5): p. 1079-1087.
6. Basu, M., S. Seggerson, J. Henshaw, J. Jiang, R. del A Cordona, C. Lefave, P.J. Boyle, A. Miller, M. Pugia, and S. Basu, *Glycoconjugate J.*, 2004. 21(8): p. 487-496.
7. Drbohlavova, J., M. Vorozhtsova, R. Hrdy, R. Kizek, O. Salyk, and J. Hubalek, *Nanoscale Res. Lett.*, 2012. 7.
8. Drbohlavova, J., J. Chomoucka, R. Hrdy, J. Prasek, L. Janu, M. Ryvolova, V. Adam, R. Kizek, T. Halasova, and J. Hubalek, *Int. J. Electrochem. Sci.*, 2012. 7(2): p. 1424-1432.
9. Prasek, J., J. Drbohlavova, J. Chomoucka, J. Hubalek, O. Jasek, V. Adam, and R. Kizek, *J. Mater. Chem.*, 2011. 21(40): p. 15872-15884.
10. Keating, C.D. and M.J. Natan, *Adv. Mater.*, 2003. 15(5): p. 451-454.
11. Eghtedari, M., A. Oraevsky, J.A. Copland, N.A. Kotov, A. Conjusteau, and M. Motamedi, *Nano Lett.*, 2007. 7(7): p. 1914-1918.
12. Prasek, J., D. Huska, O. Jasek, L. Zajickova, L. Trnkova, V. Adam, R. Kizek, and J. Hubalek, *Nanoscale Res. Lett.*, 2011. 6.
13. Hrdy, R., M. Vorozhtsova, J. Drbohlavova, J. Chomoucka, J. Prasek, J. Hubalek, and L. Tanger. *Metal 2011: 20th Anniversary International Conference on Metallurgy and Materials* 2011, Slezska: Tanger Ltd. 834-839.
14. Henderson, D. and J.Z. Wu, *J. Phys. Chem. B*, 2012. 116(8): p. 2520-2525.
15. Lee, I., K.-Y. Chan, and D. Lee Phillips, *Ultramicroscopy*, 1998. 75(2): p. 69-76.
16. Stulik, K., C. Amatore, K. Holub, V. Marecek, and W. Kutner, *Pure Appl. Chem.*, 2000. 72(8): p. 1483-1492.
17. Zoval, J.V., J. Lee, S. Gorer, and R.M. Penner, *J. Phys. Chem. B*, 1998. 102(7): p. 1166-1175.
18. Stulik, K., *Anal. Chim. Acta*, 1993. 273(1-2): p. 435-441.
19. Wang, L., J.S. Zhao, X.M. He, J.G. Ren, H.P. Zhao, J. Gao, J.J. Li, C.R. Wan, and C.Y. Jiang, *Int. J. Electrochem. Sci.*, 2012. 7(1): p. 554-560.
20. Lai, C.-M., J.-C. Lin, K.-L. Hsueh, C.-P. Hwang, K.-C. Tsay, L.-D. Tsai, and Y.-M. Peng, *Int. J. Hydrogen. Energ.*, 2007. 32(17): p. 4381-4388.
21. Hernández-Ramírez, F., A. Tarancón, O. Casals, J. Rodríguez, A. Romano-Rodríguez, J.R. Morante, S. Barth, S. Mathur, T.Y. Choi, D. Poulikakos, V. Callegari, and P.M. Nellen, *Nanotechnology*, 2006. 17(22): p. 5577.
22. Chirea, M., V. García-Morales, J.A. Manzanares, C. Pereira, R. Gulaboski, and F. Silva, *J. Phys. Chem. B*, 2005. 109(46): p. 21808-21817.
23. Gilliam, R.J., D.W. Kirk, and S.J. Thorpe, *Electrochem. Commun.*, 2007. 9(5): p. 875-878.
24. Lapierre-Devlin, M.A., C.L. Asher, B.J. Taft, R. Gasparac, M.A. Roberts, and S.O. Kelley, *Nano Lett.*, 2005. 5(6): p. 1051-1055.
25. De Leo, M., A. Kuhn, and P. Ugo, *Electroanal.*, 2007. 19(2-3): p. 227-236.
26. Wirtz, M. and C.R. Martin, *Adv. Mater.*, 2003. 15(5): p. 455-458.
27. Hubalek, J., R. Hrdy, and M. Vorozhtsova, *Proceedings of the Eurosensors Xxiii Conference*. 2009, Elsevier Science Bv: Amsterdam. p. 36-39.
28. Jia, Z., J. Liu, and Y. Shen, *Electrochem. Commun.*, 2007. 9(12): p. 2739-2743.
29. Klosova, K. and J. Hubalek, *Phys. Status Solidi A-Appl. Mat.*, 2008. 205(6): p. 1435-1438.
30. Ji, C. and P.C. Searson, *J. Phys. Chem. B*, 2003. 107(19): p. 4494-4499.
31. Erdem, A., F. Kuralay, H.E. Cubukcu, G. Congur, H. Karadeniz, and E. Canavar, *Analyst*, 2012. 137(17): p. 4001-4004.
32. Häkkinen, H., R.N. Barnett, and U. Landman, *J. Phys. Chem. B*, 1999. 103(42): p. 8814-8816.
33. Sarac, A.S., M. Ates, and B. Kilic, *Int. J. Electrochem. Sci.*, 2008. 3(7): p. 777-786.
34. Klosova, K., N. Serrano, O. Salyk, and L. Trnkova, *Curr. Nanosci.*, 2011. 7(6): p. 984-994.
35. Chang, J.H., J. Park, Y.K. Pak, J.J. Pak, and Ieee. *2007 3rd International IEEE/EMBS Conference on Neural Engineering, Vols 1 and 2* 2007. 572-574.
36. Skale, S., V. Dolecek, and M. Slemnik, *Corros Sci*, 2007. 49(3): p. 1045-1055.

37. Ren, X., F. Tang, R. Liao, and L. Zhang, *Electrochim. Acta.*, 2009. 54(28): p. 7248-7253.
38. Trnkova, L., M. Studnickova, and E. Palecek, 1980. 7(4): p. 643-658.
39. Palecek, E., F. Jelen, and L. Trnkova, 1986. 5(3): p. 315-329.
40. Oliveira-Brett, A.M., L.A. da Silva, and C.M.A. Brett, *Langmuir*, 2002. 18(6): p. 2326-2330.
41. Zhang, X., X. Liang, M. Xu, X. Bao, F. Wang, and Z. Yang, *J Appl Electrochem*, 2012. 42(6): p. 375-381.
42. Arguelho, M., J. Alves, N.R. Stradiotto, V. Lacerda, J.M. Pires, and A. Beatriz, *Quim. Nova*, 2010. 33(6): p. 1291-1296.
43. Zhang, X., D. Li, L. Bourgeois, H. Wang, and P.A. Webley, *Chem. Phys. Chem.*, 2009. 10(2): p. 436-441.
44. Li, C.Z., Y.L. Liu, and J.H.T. Luong, *Anal Chem*, 2005. 77(2): p. 478-485.
45. Adekunle, A.S., J.G. Ayenimo, X.Y. Fang, W.O. Doherty, O.A. Arotiba, and B.B. Mamba, *Int. J. Electrochem. Sci.*, 2011. 6(7): p. 2826-2844.
46. Prasek, J., L. Trnkova, I. Gablech, P. Businova, J. Drbohlavova, J. Chomoucka, V. Adam, R. Kizek, and J. Hubalek, *Int. J. Electrochem. Sci.*, 2012. 7(3): p. 1785-1801.